Ishiwa *et al. Geosci. Lett. (2016) 3:33*
DOI 10.1186/s40562-016-0065-0

Geoscience Letters

RESEARCH LETTER

Open Access

Sedimentary environmental change induced from late Quaternary sea-level change in the Bonaparte Gulf, northwestern Australia

Takeshige Ishiwa[1,2*], Yusuke Yokoyama[1,2*], Yosuke Miyairi[1], Minoru Ikehara[3] and Stephen Obrochta[4]

Abstract

Low-latitude continental shelves, mixed siliciclastic–carbonate sedimentary systems, provide an understanding of sedimentary environments driven by paleoclimatological processes. The Bonaparte Gulf, northwestern Australian continental shelf, is among the widest in the world, ranging to 500 km, with shallow carbonate terraces and platforms that were exposed during periods of lower sea level. The dominant sediments type switches between carbonate and siliciclastic over a sea-level cycle. However, the mechanism of sedimentary environmental change in the Bonaparte Gulf is not clearly understood. Here, we present a record of sedimentary environmental change from ca. 24 to 35 ka that is related to sea-level variability and exposure of carbonate terraces and platforms. Multi-proxy data from a marine sediment core show a sea-level change induced switch in sedimentary environment from siliciclastic to carbonate-dominated sedimentation during the last glaciation. Radiocarbon ages constrain the timing of this switch to ca. 26 ka, associated with a local sea-level fall of −90 m.

Keywords: Sedimentary environment, Radiocarbon dating, Bonaparte Gulf, Northwestern Australia, Last Glacial Maximum, Sea-level change

Background

Continental shelves are the main transport pathway of sediments from land to sea, playing an important role in the earth's surface system. The sedimentary environment of low-latitude mixed siliciclastic–carbonate continental shelves is strongly influenced by sea-level change and fluvial processes (Dunbar and Dickens 2003; Schlager et al. 1994; Webster et al. 2012). Detailed research on sedimentary environments of continental shelves improves our understanding of monsoonal intensity and sea-level variability (Bourget et al. 2012; Yokoyama et al. 2000).

The Bonaparte Gulf, northwestern Australia, is a broad continental shelf with a water depth shallower than ~200 m (Bourget et al. 2013, 2014). The area of the shelf has varied with relative sea-level change during the late Quaternary (Yokoyama et al. 2001a). There are several carbonate terraces and platforms such as Londonderry, Sahul, and van Diemen Rise in the Bonaparte Gulf, which were exposed during sea-level lowstands (Fig. 1; Bourget et al. 2013, 2014; van Andel et al. 1967). Carbonate terraces and platforms contain incisions at depths exceeding 100 m, connecting the Timor Sea and Bonaparte Basin (Courgeon et al. 2016). Siliciclastic sediments, transported by monsoon-influenced fluvial activity, dominate the near-shore region (Fig. 1; De Deckker et al. 2014; Nicholas et al. 2014). Shallow sediment cores show that past relative sea level fell to ~ −120 m in the Bonaparte Gulf during the Last Glacial Maximum (LGM; ~20 ka) (De Deckker and Yokoyama 2009; Ishiwa et al. 2016; Yokoyama et al. 2000, 2001b; Nakada et al. 2016).

Today, northwestern Australia experiences a semi-arid climate. Southeast winds prevail in the Austral summer and northwesterly winds in the Austral winter. There is a strong rainfall seasonality during the Austral summer (De Deckker et al. 2014; Gallagher et al. 2014a). This is the Australian monsoon, the intensity of which has

*Correspondence: t_ishiwa@aori.u-tokyo.ac.jp; yokoyama@aori.u-tokyo.ac.jp
[1] Atmosphere and Ocean Research Institute, The University of Tokyo, 5-1-5 Kashiwanoha, Kashiwa, Chiba 277-8564, Japan
Full list of author information is available at the end of the article

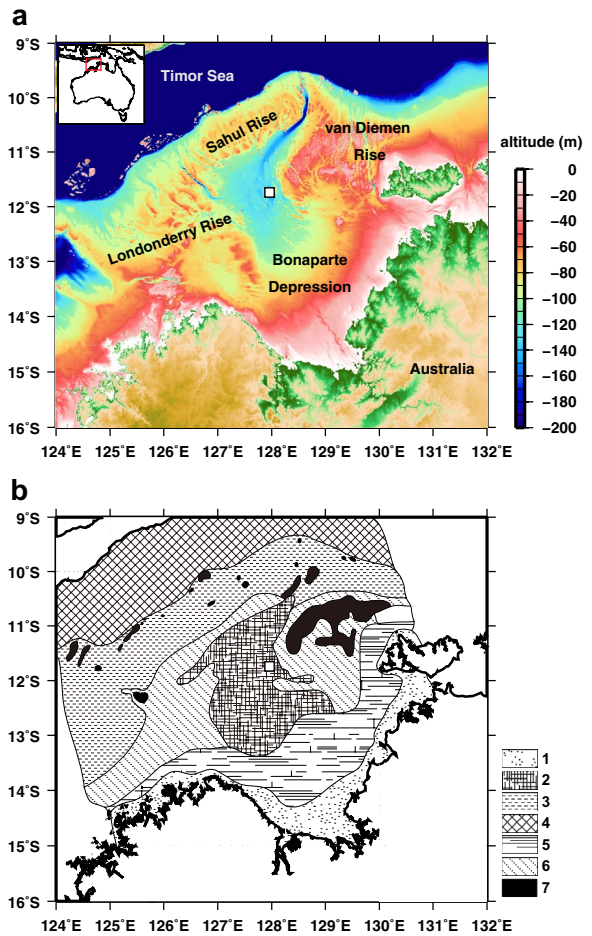

Fig. 1 Bonaparte Gulf, northwestern Australia. **a** The location of core site KH11-1-PC01 (*white square*), bathymetry and named seabed features are referred to in the text. Bathymetric data is from Whiteway (2009). **b** Distribution of surface sediments, modified from van Andel et al. (1967). *1* recent near-shore sediments, *2* calcareous silty clays of Bonaparte Depression, *3* shelf-edge foraminiferal calcilutites and calcarenites, *4* Timor Trough silty clay and calcilutites, *5* relict transgressive quartzose calcarenites, *6* relict transgressive calcarenites, *7* bank facies. Legends refer to van Andel et al. (1967)

varied with the movement of the Intertropical Convergence Zone (ITCZ) over the past 30,000 years (cf., Ding et al. 2013; Kuhnt et al. 2015; Mohtadi et al. 2011).

This mixed siliciclastic–carbonate and shallow continental shelf is influenced by monsoonal intensity and sea-level change (Gallagher et al. 2014b). Petroleum exploration and paleoclimatic reconstructions have driven interest in the long-term understanding of the sedimentary environment in this region (Anderson et al. 2011; Nicholas et al. 2014). Moreover, mixed siliciclastic–carbonate sedimentary environments in low-latitude and semi-enclosed marginal marine environments provide information on the mechanism of paleoclimatic and hydrologic change (cf., Bahr et al. 2005; Isaack et al. 2016; Soulet et al. 2011). However, our understanding of late Quaternary evolution of the Bonaparte sedimentary environment is much less well constrained.

Here, we document the evidence of environmental changes due to the exposure of these carbonate terraces and platforms before the LGM. The Bonaparte Gulf is a "far-field" (cf., Yokoyama and Esat 2011), tectonically stable site extremely suitable for reconstruction of sea level due to past continental ice-volume change (De Deckker and Yokoyama 2009; Ishiwa et al. 2016; Yokoyama et al. 2000, 2001b). We also describe the sedimentary consequences of past environmental change from a marine piston core (KH11-1-PC01) using Ca/Ti ratios, total organic carbon (TOC) and total nitrogen (TN), constrained by radiocarbon dating.

Methods

Materials

Core KH11-1-PC01 was recovered from a water depth of 140 m during the KH11-1 cruise of R/V Hakuho-Maru during January and February 2011 (Fig. 1). The top 600 cm interval of core KH11-1-PC01 (core recovery length: 951 cm) was analyzed as it is within the range of radiocarbon dating. Well-preserved macrofossils (primarily bivalves) were collected for radiocarbon dating.

Physical properties and geochemical analysis

Color reflectance was measured at 2-cm intervals after splitting the cores on ship using a Minolta CM-2002 photospectrometer. At the same time, magnetic susceptibility was measured at 2-cm intervals using a Bartington Instruments MS2C system.

TOC and TN were measured using an EA-IRMS (Elemental Analysis-Isotope Ratio Mass Spectrometry: Flash EA 1112 and Delta plus Advantage) at the Center for Advanced Marine Core Research, Kochi University, Japan (cf., Ishiwa et al. 2016; Nakamura et al. 2016; Riethdorf et al. 2015). Bulk sediments were treated with 3 M HCl to remove inorganic carbonate. Split-core scanning X-ray fluorescence (XRF) analysis was later conducted at a 1-cm interval using the TATSCAN-F2 at the Center for Advanced Marine Core Research (Sakamoto et al. 2006). The XRF core scanner analysis was affected by split-core surface condition and water content, especially for the light elements (Kido et al. 2006; Nakamura et al. 2016). Hence, we discuss the variation of relatively heavy elements, calcium (Ca), and titanium (Ti). The flux of Ca and Ti is calculated as follows,

$$\mathrm{MAR} = \mathrm{DBD} \times \mathrm{LSR}$$

$$\mathrm{Ca(Ti)flux} = \mathrm{MAR} \times \mathrm{Ca(Ti)(counts)}$$

where MAR is the mass accumulation rate (g/cm^2 year), DBD is the dry bulk density (g/cm^2), and LSR is the linear sedimentation rate (cm/year).

Radiocarbon dating was performed on marine macrofossils (Table 1) and bulk sediment organic matter. Macrofossils were etched by 10 M HCl to remove secondary and contaminating calcium carbonate (Yokoyama et al. 2016a). Bulk sediments were pretreated twice in 3 M HCl for 12 h to digest inorganic calcium carbonate (Ishiwa et al. 2016). We followed the methods of Yokoyama et al. (2007) in the graphitization and measured the graphite by the Single Stage Accelerator Mass Spectrometry (Yokoyama et al. 2016b) and the Micro Analysis Laboratory Tandem Accelerator at the University of Tokyo.

Age–depth model

Calendar ages were calculated using Oxcal (Ramsey and Lee 2013) with Marine 13 and Intcal 13 (Reimer et al. 2013) as calibration curves for macrofossils and organic matter ages. The local reservoir correction, ΔR, is undefined in the Bonaparte Gulf but expected to be minor (cf., O'Connor et al. 2010). Thus, we made no local correction, consistent with previous works (Ishiwa et al. 2016; Yokoyama et al. 2000, 2001b).

The age–depth model of KH11-1-PC01 was constrained using the BACON model (Blaauw and Christen 2011) based on macrofossil ages, since organic matter ages are affected by the transportation time of terrigenous components (cf., Ishiwa et al. 2016; Nakamura et al. 2016). This model uses the Bayesian analysis and Monte Carlo methods to constrain the smoothing age–depth model using the R statistical software package (cf., De Vleeschouwer et al. 2012; Shanahan et al. 2012).

Calculation for exposure percentage in the Bonaparte Gulf

The area of carbonate terraces and platforms in the Bonaparte Gulf exposed during lower sea level was calculated using the bathymetric dataset from Whiteway (2009). The data were interpolated to a uniform resolution of 0.5 min latitudinally and longitudinally. We calculated the area of exposure along the sea-level curve and set the exposure percentage to 0% at relative sea level = 0 m and to 100% at relative sea level = −120 m. This percentage was calculated at a 5-m interval.

Results

Lithology and physical properties

The interval from 600 to 560 cm of core KH11-1-PC01 is silty clay with mm-scale shell fragments. Fine sand is present from 560 to 520 cm and silty clay occurs from 520 to 510 cm with shell fragments, foraminifers and nannofossils (as noted in shipboard smear slides). Fine sand is present from 510 to 490 cm and silty clay with shell fragments, and nannofossils from 490 to 60 cm. The upper 60 cm of core is silt and clay with shell fragments and bioturbation. Color reflectance (b*) values gradually increase from 1 to 9 in the uppermost 300 cm with a slight shift at 200 cm, indicating an increasing yellow component. A relatively large increase in b* occurs at 30 cm (Fig. 2). Magnetic susceptibility (MS) shows a slight decrease from 7 to 4 SI 10^{-6} at 200 cm with a maximum of 11 SI 10^{-6} at 10 cm. In the upper 10 cm, the MS decreases to 0 SI 10^{-6} (Fig. 2).

Table 1 Age results of macrofossils in core KH11-1-PC01

Lab. No.	Material	Depth (cm)	^{14}C age (BP)	Calendar age (cal BP) 1σ	Calendar age (cal BP) 2σ
YAUT-01960	Bivalves	1	2320 ± 30	1940 ± 40	1940 ± 90
YAUT-01960	Bivalves	3	10,510 ± 40	11,730 ± 140	11,670 ± 260
YAUT-01960	Bivalves	22	9750 ± 40	10,650 ± 50	10,660 ± 110
YAUT-01960	Bivalves	31	18,370 ± 50	21,770 ± 100	21,750 ± 200
B274	Coral	43	590 ± 130	200 ± 140	–
YAUT-01961	Bivalves	64	20,290 ± 70	23,930 ± 120	23,920 ± 250
YAUT-01961	Bivalves	74	20,290 ± 70	23,940 ± 120	23,930 ± 250
YAUT-01961	Bivalves	133	20,940 ± 70	24,710 ± 180	24,730 ± 320
B274	Bivalves	166	20,950 ± 140	24,740 ± 240	24,760 ± 430
YAUT-01964	Bivalves	173	20,910 ± 70	24,660 ± 170	24,690 ± 310
B274	Bivalves	217	23,320 ± 210	27,270 ± 200	27,160 ± 450
YAUT-01961	Bivalves	218	23,280 ± 70	27,250 ± 100	27,240 ± 200
YAUT-01962	Bivalves	291	24,280 ± 90	27,890 ± 100	27,920 ± 220
B274	Barnacle	368	25,330 ± 280	28,990 ± 300	29,020 ± 610
B274	Gastropod	560	30,060 ± 230	33,820 ± 190	33,820 ± 410
B274	Bivalves	603	35,020 ± 550	39,160 ± 580	39,270 ± 1280

Data are calculated by Marine13 (Reimer et al. 2013). "YAUT-" is a laboratory number of the Single Stage Accelerator Mass Spectrometry at the University of Tokyo. "B274" is a laboratory number of the Micro Analysis Laboratory Tandem Accelerator at the University of Tokyo

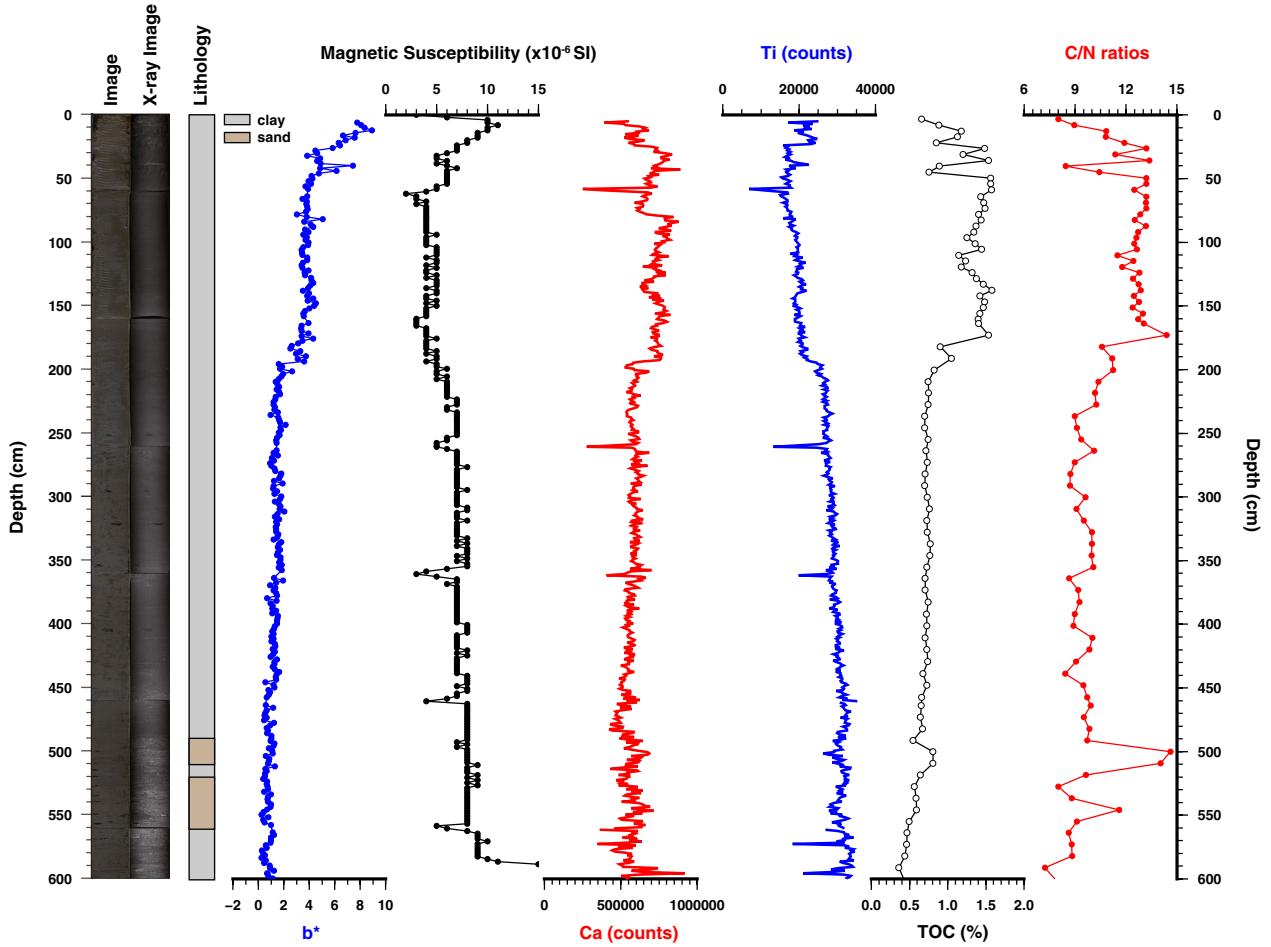

Fig. 2 Image of core KH11-1-PC01, X-ray image, lithology, color reflectance (b*), magnetic susceptibility, Ca, Ti, TOC, and C/N ratios

XRF core scanning and geochemical analysis

Ca counts are constant at 600,000 from 600 to 200 cm, increasing to ~800,000 counts at 180 cm (Fig. 2). There is a sharp drop at 70 cm. From 30 cm to the core top, Ca decreases to 400,000 counts. Ti counts gradually decrease from 600 to 200 cm, sharply decreasing to 20,000 counts at ~200 cm (Fig. 2). There is a peak of ~25,000 counts from 30 cm to the core top.

TOC is ~0.7% from 600 to 200 cm, sharply increasing to 1.5% at ~180 cm with a peak of ~0.8% at ~510 cm (Fig. 2). TOC is variable in the upper 40 cm of core. C/N ratios reach a maximum of ~15 at 510 cm, then maintain a value of ~9 through the depth interval of 500–180 cm, above which values are relatively constant at ~13 (Fig. 2). In the upper 60 cm, ratios decrease upwards to the core top.

Radiocarbon dating

Tables 1 and 2 summarize the results of radiocarbon dating and Fig. 3 shows the age–depth relationship. Macrofossils dates show the range from ca. 35 to 24 ka and bulk organic matter from ca. 37 to 25 ka during the interval of 600–60 cm. The upper 60 cm is either disturbed by coring or winnowed by tidal currents (http://www.bom.gov.au/australia/tides/) and pockmark activity (Nicholas et al. 2014), and the ages in this interval are not interpreted here (Fig. 3). Below 60 cm, the age–depth model is well constrained with an offset between macrofossils and organic matter ages (cf., Ishiwa et al. 2016). The average value of this offset is ~800 ^{14}C year within the period from ca. 35 to 25 ka and ~1200 ^{14}C year with the period from ca. 25 to 24 ka. The average sedimentation rate is 0.47 m/kyr for the period from ca. 35 to 25 ka and 0.75 m/kyr for the period from ca. 25 to 24 ka.

Exposure of carbonate terraces and platforms in Bonaparte Gulf

Figure 4a shows the calculated percentage of exposure and the rate of sea-level change from 0 to −120 m in 5 m increments. During sea-level lowstands, the proportion

Table 2 Age results of organic matter in core KH11-1-PC01

Lab. No.	Depth (cm)	^{14}C age (BP)	Calendar age (cal BP) 1σ	Calendar age (cal BP) 2σ
YAUT-003718	3	1790 ± 30	1700 ± 80	1720 ± 100
YAUT-003906	22	7650 ± 30	8430 ± 20	8450 ± 60
YAUT-003719	45	7040 ± 70	7870 ± 70	7840 ± 140
YAUT-012705	54	21,040 ± 80	25,400 ± 120	25,390 ± 230
YAUT-003907	74	21,450 ± 60	25,780 ± 80	25,770 ± 150
YAUT-004007	101	21,180 ± 70	25,540 ± 110	25,510 ± 220
YAUT-003720	133	22,200 ± 110	26,390 ± 170	26,440 ± 350
YAUT-003721	173	21,780 ± 100	26,000 ± 90	26,010 ± 200
YAUT-003722	218	25,060 ± 110	29,090 ± 170	29,110 ± 320
YAUT-014534	255	24,370 ± 90	28,440 ± 150	28,420 ± 280
YAUT-004008	291	25,090 ± 90	29,120 ± 160	29,140 ± 300
YAUT-003723	369	26,360 ± 130	30,700 ± 150	30,660 ± 300
YAUT-003724	555	30,600 ± 150	34,560 ± 170	34,530 ± 330
YAUT-003725	600	32,810 ± 200	36,720 ± 330	36,930 ± 680

Data are calculated by Intcal 13 (Reimer et al. 2013). "YAUT-" is a laboratory number of the Single Stage Accelerator Mass Spectrometry at the University of Tokyo

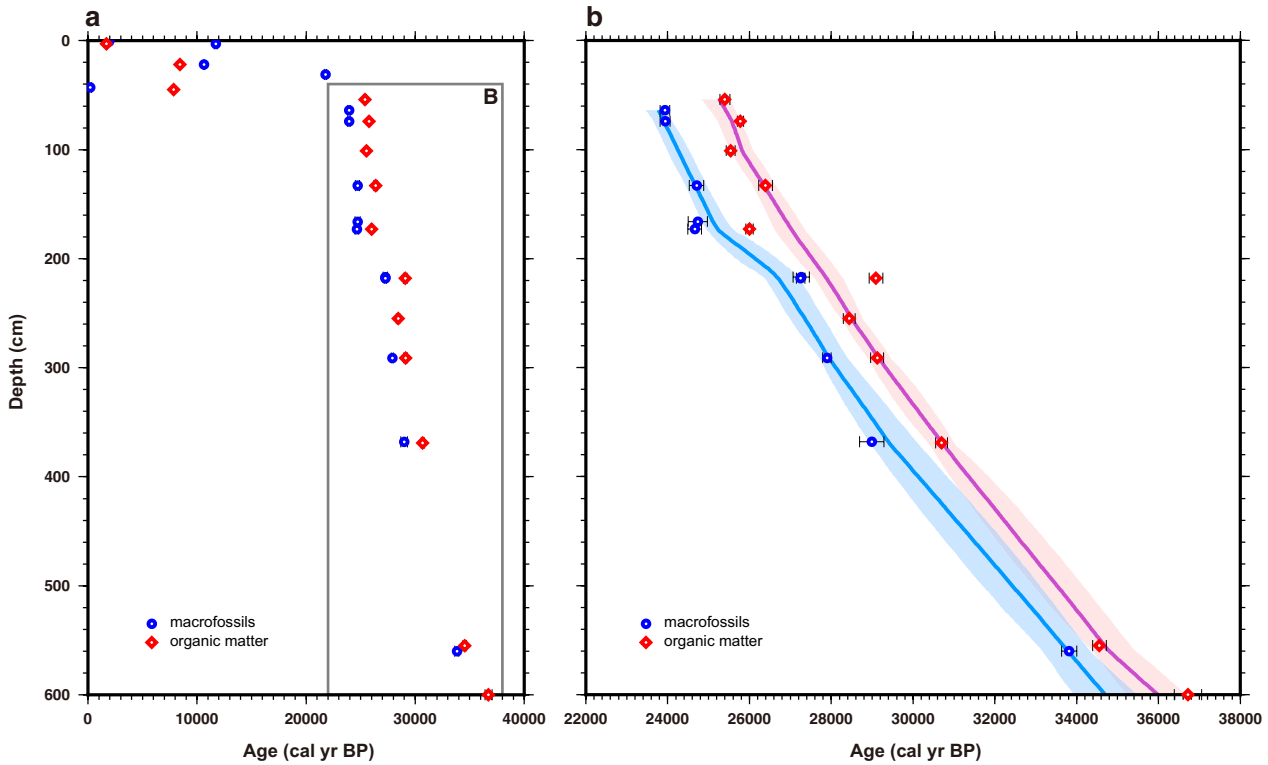

Fig. 3 The age–depth relationship of core KH11-1-PC01. **a** Calendar ages for macrofossils (*blue*) and organic matter (*red*). The errors are 2 sigma. **b** Expanded view of the age–depth model in 22–38 ka. The *line* is the mean value of the BACON model (Blaauw and Christen 2011) and the *shade* represents the minimum and maximum range of the BACON model

of carbonate terraces and platforms exposed in Bonaparte Gulf ranged from 25% when sea level was at −60 m to in excess of 90% when sea level fell below −100 m. The rate of change from −70 to −90 m is greater than 1.5%/m. The maximum rate of change is at −80 m (Fig. 4b).

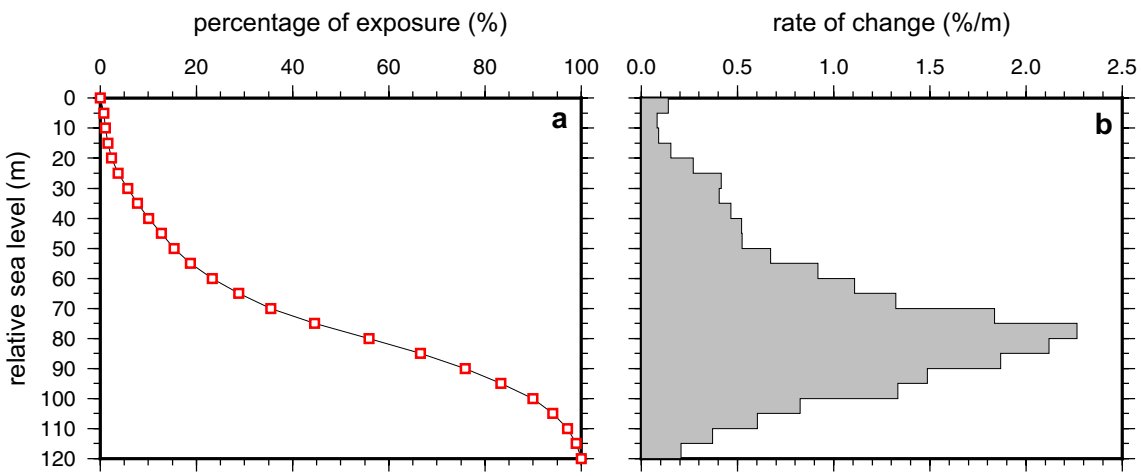

Fig. 4 **a** Proportion (%) of carbonate platform area in Bonaparte Gulf exposed at lower sea levels; **b** rate of change in proportional area of the platforms exposed at sea level fall

Interpretation and discussion

Sedimentary environmental change during late Quaternary

Biogenic or precipitated carbonate shows high Ca-intensities with an inverse relationship to K-, Fe-, Mn-, and Ti- intensities that are correlated with siliciclastic components (cf., Bahr et al. 2005; Kuhnt et al. 2015). Ca/Ti, Ca/K, Ca/Mn and Ca/Fe all exhibit a similar pattern of variability (see Additional file 1: Figure S1). Thus, we focus on Ca/Ti, which is less sensitive to redox changes. We suggest that calcium variation represents changes in biogenetic carbonate flux from the carbonate terraces and platform of the Bonaparte Gulf (Fig. 5; and see Additional file 1: Figure S2). The Ca flux after 25 ka is much higher than before 27 ka, indicating a carbonate flux increase caused by exposure of the carbonate platforms during lower sea level at ca. 26 ka (190 cm) (Fig. 5). In addition, we use the titanium variation to represent terrigenous sediment flux, derived from clay minerals (cf., Gingele et al. 2001; Gingele and De Deckker 2003). Magnetic susceptibility values decrease from 27 to 25 ka (Fig. 6). This pattern likely reflects the dilution by sediments dominated by biogenetic carbonate with low magnetic susceptibility.

The variation in terrigenous input is interpreted to be related to changes in TOC flux and C/N ratios (cf., Ishiwa et al. 2016; Yu et al. 2010; Mackie et al. 2005). The terrigenous sediment supply increased after ca. 26 ka, as indicated by the increased TOC, C/N ratios, and sedimentation rate (Figs. 5, 6). Increased terrigenous material during this time would make mixed marine-terrigenous organic matter older, increasing the offset from macrofossil ages (Fig. 3). Additionally, mass accumulation rate calculated by the BACON model supports the exposure of carbonate terraces and platforms during this period (Fig. 5).

Mechanism for sedimentary environmental change

The carbonate terraces and platforms of the outer Bonaparte Gulf are dissected by a network of deeply incised paleochannels that would have provided sediment transport pathways during lower sea level (Courgeon et al. 2016; Fig. 7; see also Additional file 1: Figure S3). Yokoyama et al. (2000, 2001b) estimated the age of deposition in these paleochannels to be ca. 17.5 ka, suggesting that carbonate sediments were produced and transported to the depression during lower sea level by fluvial activity or ocean currents.

Sedimentation patterns would have fluctuated with the relative strength of monsoon (Gallagher et al. 2014b; Kuhnt et al. 2015). The Australian Monsoonal precipitation pattern is sensitive to latitudinal ITCZ migration (Lewis et al. 2011), while speleothem records from this region indicate low monsoon variability at this time (Lewis et al. 2011; Partin et al. 2007), consistent with marine and terrestrial records (Fitzsimmons et al. 2013; Reeves et al. 2013) that show a northward ITCZ position. We suggest that the changes in monsoonal variability are not strong enough to control the sedimentary facies in the Bonaparte Gulf. A relative change in carbonate sediment flux increased at ca. 26 ka as shown by physical properties and geochemical analysis (Fig. 5). Rivers passing through the continent would have supplied siliciclastic sediments to the depression (Gingele et al. 2001;

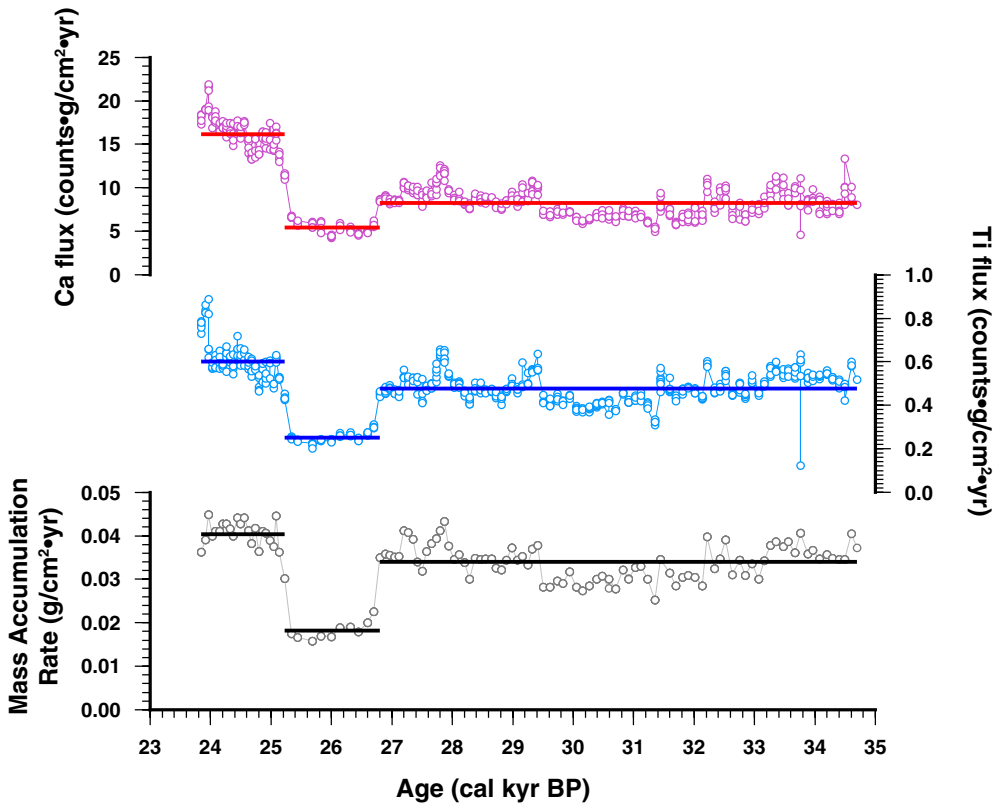

Fig. 5 Ca flux, Ti flux, and mass accumulation rate. *Solid lines* correspond to the average values during three periods, before ~27 ka, during 25–27 ka, and after ~25 ka

Gingele and De Deckker 2003). During this period, the supply of siliciclastic sediments did not change much due to the weak variability of monsoonal intensity. By contrast, the carbonate supply increased due to the exposure of carbonate terraces and platforms.

Sea level below −90 m resulted in sufficient exposure of carbonate terraces and platform to increase the flux of carbonate sediments (Fig. 7). During sea-level highstands, much of the shelf was submerged. During sea-level lowstands, the carbonate terraces and platforms were exposed and the Bonaparte Depression was semi-enclosed from the Timor Sea. The relative area of exposure was an important control on the sedimentary facies of the gulf.

While the hydro-isostatic effects in the Bonaparte Gulf do not significantly affect to the current interpretation (Yokoyama et al. 2000, 2001b), this factor cannot be entirely discounted due to paleotopography and paleo-water depth effects. Yokoyama et al. (2000, 2001b) estimated the amplitude of this effect (offset between the global sea level and relative sea level) is less than 20 m. Therefore, the bathymetry in Fig. 7 has an error of 10% due to hydro-isostasy effects.

These observations indicate that the sedimentary environment in the Bonaparte Gulf is primarily driven by sea-level variability due to the distinctive topography with its central depression surrounded by higher-level carbonate terraces and platforms. Exposure of carbonate terraces and platforms with a sea-level fall enhances sedimentary environmental change, characterized by carbonate sediment production and transportation. Paleobathymetry would also likely have affected local ocean circulation patterns and tidal ranges.

Sea-level change prior to the LGM has been estimated using the uplifted coral on the Huon Peninsula, indicating that sea level fell from −70 to −110 m from 30 to 24 ka (Cutler et al. 2003; Yokoyama et al. 2001c). This is consistent with sea level from the Red Sea (Siddall

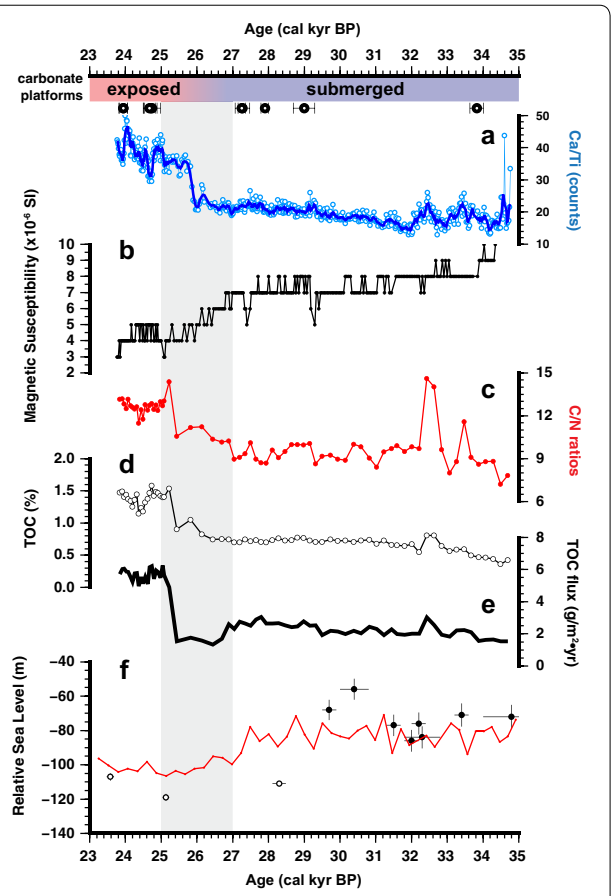

Fig. 6 Ca/Ti, magnetic susceptibility, C/N ratios, TOC, TOC flux, and sedimentation rate, and relative sea-level records. *Gray shade* corresponds to the timing of carbonate platform exposure due to sea-level fall. *A* Ca/Ti. *B* Magnetic susceptibility. *C* C/N ratios. *D* TOC (%). *E* TOC flux. *F* Relative sea-level records in Huon Peninsula. *Black circles* correspond to Yokoyama et al. (2001c). *White circles* to Cutler et al. (2003). *Red line* to Siddall et al. (2003)

et al. 2003), which falls ~20 m from 28 to 26 ka (−80 to −100 m).

Comparison to other regions

Mixed carbonate-siliciclastic sedimentary systems are observed in low-latitude tropical regions. Isaack et al. (2016) present a sea-level driven model of sediment dynamics based on a multi-proxy record in the barrier-reef lagoon of Bora Bora in the South Pacific. They suggest that carbonate sediment produced in marginal reef areas is transported to the lagoons. This mechanism indicates that carbonate terraces and platforms in the Bonaparte Gulf can be the source of carbonate sediments, generating the variation of geochemical signal in the core.

The Black Sea became a semi-enclosed marginal sea, similar to the Bonaparte Gulf, during lowering sea levels (Bahr et al. 2005), and reconnected to the Mediterranean Sea at ~9000 years ago in association with rising sea level (Soulet et al. 2011). Geochemical data suggest that the hydrologic system has changed from lacustrine to marine, controlled by a water depth of sills connected to Mediterranean Sea. By contrast, during sea-level lowstands, the Bonaparte Gulf connected to the Timor Sea mainly by paleochannels at a water depth of ~200 m (Fig. 1; Yokoyama et al. 2000, 2001a). The sedimentary environment in the Bonaparte Gulf is influenced by the exposure of carbonate terraces and platforms, which played a role in pathways of carbonate sediments.

Conclusions

Geochemical and chronological records from a piston core in the Bonaparte Gulf, northwestern Australia, show a sedimentary environmental change at ca. 26 ka. Carbonate terraces and platforms and their deeply incised paleochannels play an important role in this paleoenvironmental change.

Ca/Ti ratios as an indicator of changes in mixed siliciclastic–carbonate sediments increased at ca. 26 ka, indicating the enhanced supply of carbonate sediments. TOC and C/N ratios as an indicator of terrigenous input also increased. The changes in these geochemical signals can be explained by the exposure of carbonate terraces and platforms.

Precipitation patterns shift can drive the change in sediment supply. However, during the period we investigate, the variability of Australian monsoon was not strong enough to change the sedimentary environment. By contrast, global sea-level fall to −90 m occurred at ca. 26 ka, driving the exposure of carbonate terraces and platforms and the switch from siliciclastic to carbonate-dominated sedimentation. Our research provides an understanding of a sea-level driven sedimentary environmental change in low-latitude mixed siliciclastic–carbonate environment.

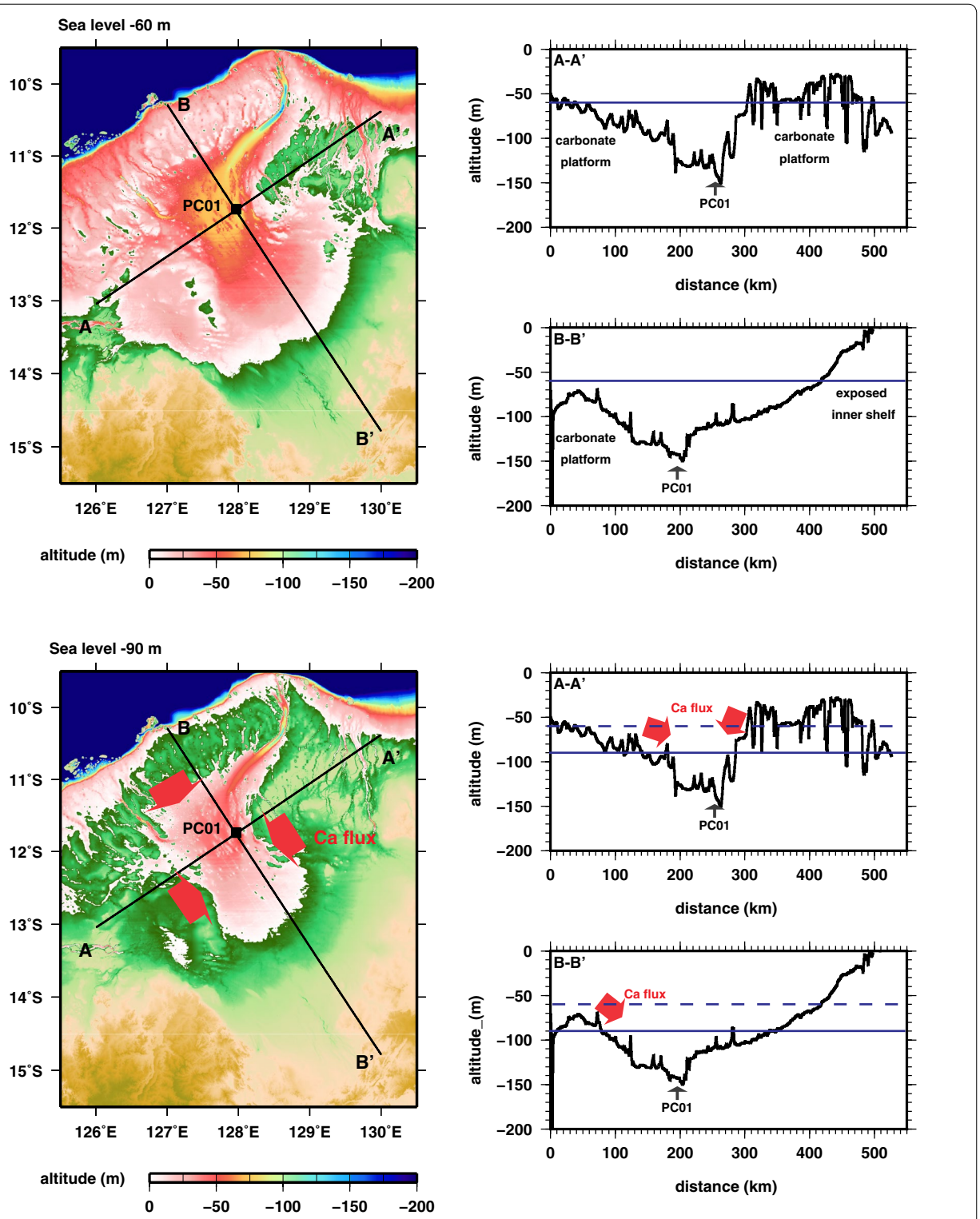

Fig. 7 Bathymetry and sectional views of the Bonaparte Gulf at −60 and −90 m sea level. Note that there are bathymetric error estimates in the Bonaparte Gulf due to the hydro-isostatic effect (Yokoyama et al. 2000, 2001a, b). The effects are relatively minor

Additional file

Additional file 1. Additional figures.

Abbreviations

ITCZ: Intertropical Convergence Zone; LGM: last glacial maximum; TOC: total organic carbon; TN: total nitrogen; MAR: mass accumulation rate; DBD: dry bulk density; LSR: liner sedimentation rate; XRF: X-ray fluorescence; MS: magnetic susceptibility.

Authors' contributions

TI carried out this work and YY managed the cruise KH11-1 and also supervised this work. YM supported measurement of this work. MI managed measurement in CMCR and gave useful comments. SO interpreted results and helped to write the final manuscript. YY, YM, MI and SO joined the cruise of KH11-1. All authors read and approved the final manuscript.

Author details

[1] Atmosphere and Ocean Research Institute, The University of Tokyo, 5-1-5 Kashiwanoha, Kashiwa, Chiba 277-8564, Japan. [2] Department of Earth and Planetary Science, Graduate School of Science, The University of Tokyo, 7-3-1 Hongo, Bunkyo, Tokyo 113-0033, Japan. [3] Center for Advanced Marine Core Research, Kochi University, B200 Monobe, Nankoku, Kochi 783-8502, Japan. [4] Faculty of International Resource Science, Akita University, 1-1 Tegata-Gakuenmachi, Akita, Akita 010-8502, Japan.

Acknowledgements

We greatly appreciate the members of the cruise of KH11-1 for collecting and subsampling the sediment cores. The reviewers, Dr. S. Nichol and Dr. S. Gallagher, gave us the useful and valuable comments to revise this paper. This study was supported by the Center for Advanced Marine Core Research (CMCR), Kochi University, cooperative research program (11A031, 11B039) and grants from the Japan Society for the Promotion of Science (JSPS) KAKENHI (JP26247085, JP15KK0151) and JSPS Fellows DC2 (16J04542).

Competing interests

The authors declare that they have no competing interests.

Received: 12 August 2016 Accepted: 29 November 2016
Published online: 07 December 2016

References

Anderson TJ, Nichol S, Radke L, Heap AD, Battershill C, Hughes M, Siwabessy PJ, Barrie V, Alvarez de Glasby B, Tran M, Daniell J (2011) Seabed environments of the Eastern Joseph Bonaparte Gulf, Northern Australia: GA0325/Sol5117-Post-survey Report. Geosci Aust Record

Bahr A, Lamy F, Arz H, Kuhlmann H, Wefer G (2005) Late glacial to Holocene climate and sedimentation history in the NW Black Sea. Mar Geol 214:309–322

Blaauw M, Christen JA (2011) Flexible paleoclimate age–depth models using an autoregressive gamma process. Bayesian Anal 6:457–474

Bourget J, Ainsworth RB, Backé G, Keep M (2012) Tectonic evolution of the northern Bonaparte Basin: impact on continental shelf architecture and sediment distribution during the Pleistocene. Aust J Earth Sci 59:877–897

Bourget J, Ainsworth RB, Nanson R (2013) Origin of mixed carbonate and siliciclastic sequences at the margin of a "giant" platform during the Quaternary (Bonaparte Basin, NW Australia). In: Verwer K, Playton TE, Harris PM (eds) Deposits, architecture, and controls of carbonate margin, slope, and basinal settings, special publication 105. SEPM (Society for Sedimentary Geology), Tulsa

Bourget J, Ainsworth RB, Thompson S (2014) Seismic stratigraphy and geomorphology of a tide or wave dominated shelf-edge delta (NW Australia): process-based classification from 3D seismic attributes and implications for the prediction of deep-water sands. Mar Pet Geol 57:359–384

Courgeon S, Bourget J, Jorry SJ (2016) A Pliocene—Quaternary analogue for ancient epeiric carbonate settings: the Malita intrashelf basin (Bonaparte Basin, northwest Australia). AAPG Bull 100:565–595

Cutler KB, Edwards R, Taylor FW, Cheng H, Adkins J, Gallup C, Cutler PM, Burr GS, Bloom AL (2003) Rapid sea-level fall and deep-ocean temperature change since the last interglacial period. Earth Planet Sci Lett 206:253–271

De Deckker P, Yokoyama Y (2009) Micropalaeontological evidence for Late Quaternary sea-level changes in Bonaparte Gulf, Australia. Global Planet Chang 66:85–92

De Deckker P, Barrows TT, Rogers J (2014) Land e sea correlations in the Australian region: post-glacial onset of the monsoon in northwestern Western Australia. Quat Sci Rev 105:181–194

De Vleeschouwer F, Pazdur A, Luthers C, Streel M, Mauquoy D, Wastiaux C, Le Roux G, Moschen R, Blaauw M, Pawlyta J, Piotrowska N (2012) A millennial record of environmental change in peat deposits from the Misten bog (East Belgium). Quat Int 268:44–57

Ding X, Bassinot F, Guichard F, Fang NQ (2013) Marine Micropaleontology Indonesian Through flow and monsoon activity records in the Timor Sea since the last glacial maximum. Mar Micropaleontol 101:115–126

Dunbar GB, Dickens GR (2003) Massive siliciclastic discharge to slopes of the Great Barrier Reef Platform during sea-level transgression: constraints from sediment cores between 15°S and 16°S latitude and possible explanations. Sed Geol 162:141–158

Fitzsimmons KE, Cohen TJ, Hesse PP, Jansen J, Nanson GC, May J, Barrows TT, Haberlah D, Hilger A, Kell T, Larsen J, Lomax J, Treble P (2013) Late Quaternary palaeoenvironmental change in the Australian drylands. Quat Sci Rev 74:78–96

Gallagher SJ, Fulthorpe CS, Bogus KA (2014a) Reefs, oceans, and climate: a 5 million year history of the Indonesian Throughflow, Australian monsoon, and subsidence on the northwest shelf of Australia. International Ocean Discovery Program Scientific Prospectus 356

Gallagher SJ, Wallace MW, Hoiles PW, Southwood JM (2014b) Seismic and stratigraphic evidence for reef expansion and onset of aridity on the Northwest Shelf of Australia during the Pleistocene. Mar Pet Geol 57:470–481

Gingele FX, De Deckker P (2003) Fingerprinting Australia's rivers using clays and the application for the marine record of rapid climate change. Advances in Regolith. ANU Research Publications, pp 140–143

Gingele FX, De Deckker P, Hillenbrand CD (2001) Clay mineral distribution in surface sediments between Indonesia and NW Australia-source and transport by ocean currents. Mar Geol 179:135–146

Isaack A, Gischler E, Hudson JH, Anselmetti FS, Lohner A, Vogel H, Garbode E, Camoin GF (2016) A new model evaluating Holocene sediment dynamics: insights from a mixed carbonate—siliciclastic lagoon (Bora Bora, Society Islands, French Polynesia, South Pacific). Sed Geol 343:99–118

Ishiwa T, Yokoyama Y, Miyairi Y, Obrochta S, Sasaki T, Kitamura A, Suzuki A, Ikehara M, Ikehara K, Kimoto K, Bourget J, Matsuzaki H (2016) Reappraisal of sea-level lowstand during the Last Glacial Maximum observed in the Bonaparte Gulf sediments, northwestern Australia. Quat Int 397:373–379

Kido Y, Koshikawa T, Tada R (2006) Rapid and quantitative major element analysis method for wet fine-grained sediments using an XRF microscanner. Mar Geol 229:209–225

Kuhnt W, Holbourn A, Xu J, Opdyke B, De Deckker P, Mudelsee M (2015) Southern Hemisphere control on Australian monsoon variability during the late deglaciation and Holocene. Nat Commun 6:5916

Lewis SC, Gagan MK, Ayliffe LK, Zhao J, Hantoro WS, Treble PC, Hellstrom JC, LeGrande AN, Kelley M, Schmidt GA, Suwargadi BW (2011) High-resolution stalagmite reconstructions of Australian–Indonesian monsoon rainfall variability during Heinrich stadial 3 and Greenland interstadial 4. Earth Planet Sci Lett 303:133–142

Mackie EAV, Leng MJ, Lloyd JM, Arrowsmith C (2005) Bulk organic $\delta^{13}C$ and C/N ratios as palaeosalinity indicators within a Scottish isolation basin. J Quat Sci 20:303–312

Mohtadi M, Oppo DW, Steinke S, Stuut JW, De Pol-holz R, Hebbeln D, Lückge A (2011) Glacial to Holocene swings of the Australian-Indonesian monsoon. Nature Geosci 4:540–544

Nakada M, Okuno J, Yokoyama Y (2016) Total meltwater volume since the Last Glacial Maximum and viscosity structure of Earth's mantle inferred from relative sea level changes at Barbados and Bonaparte Gulf and GIA-induced J2. Geophys J Int 204:1237–1253

Nakamura A, Yokoyama Y, Maemoku H, Yagi H, Okamura M, Matsuoka H, Miyake N, Osada T, Pani Adhikari D, Dangol V, Ikehara M, Miyairi Y, Matsuzaki H (2016) Weak monsoon event at 4.2 ka recorded in sediment from Lake Rara, Himalayas. Quat Int 397:349–359

Nicholas WA, Nichol SL, Howard FJF, Picard K, Dulfer H, Radke LC, Carroll AG, Siwabessy PJW (2014) Pockmark development in the Petrel Sub-basin, Timor Sea, Northern Australia: seabed habitat mapping in support of CO_2 storage assessments. Cont Shelf Res 83:129–142

O'Connor S, Ulm S, Fallon SJ, Barham A, Loch I (2010) Pre-bomb marine reservoir variability in the Kimberley Region, Western Australia. Radiocarbon 52:1158–1165

Partin JW, Cobb KM, Adkins JF, Clark B, Fernandez DP (2007) Millennial-scale trends in west Pacific warm pool hydrology since the Last Glacial Maximum. Nature 449:452–455

Ramsey CB, Lee S (2013) Recent and planned developments of the program oxcal. Radiocarbon 55:720–730

Reeves JM, Bostock HC, Ayliffe LK, Barrows TT, De Deckker P, Devriendt LS, Dunbar GB, Drysdale RN, Fitzsimmons KE, Gagan MK, Griffiths ML, Haberle SG, Jansen JD, Krause C, Lewis S, McGregor HV, Mooney SD, Moss P, Nanson GC, Purcell A, van der Kaars S (2013) Palaeoenvironmental change in tropical Australasia over the last 30,000 years—a synthesis by the OZ-INTIMATE group. Quat Sci Rev 74:97–114

Reimer PJ, Bard E, Bayliss A, Beck JW, Blackwell PG, Ramsey CB, Buck CE, Cheng H, Edwards RL, Friedrich M, Grootes PM, Guilderson TP, Haflidason H, Hajdas I, Hatte C, Heaton TJ, Hoffmann DL, Hogg AG, Hughen KA, Kaiser KF, Kromer B, Manning SW, Niu M, Reimer RW, Richards DA, Scott EM, Southon JR, Staff RA, Turney CSM, van der Plicht J (2013) Intcal13 and marine13 radiocarbon age calibration curves 0–50,000 years cal bp. Radiocarbon 55:1869–1887

Riethdorf JR, Thibodeau B, Ikehara M, Nurnberg D, Max L, Tiedemann R, Yokoyama Y (2015) Surface nitrate utilization in the Bering sea since 180kA BP: insight from sedimentary nitrogen isotopes. Deep Sea Res Part II Top Stud Oceanogr:1–14

Sakamoto T, Kuroki K, Sugawara T, Aoike K, Iijima K, Sugisaki S (2006) Non-destructive X-Ray fluorescence (XRF) core-imaging scanner, TATSCAN-F2. Sci Drill 2:37–39

Schlager W, Reijmer JJG, Droxler A (1994) Highstand shedding of carbonate platforms. J Sediment Res B64:270–281

Shanahan TM, Beck JW, Overpeck JT, McKay NP, Pigati JS, Peck JA, Scholz CA, Heil CW, King J (2012) Late Quaternary sedimentological and climate changes at Lake Bosumtwi Ghana: new constraints from laminae analysis and radiocarbon age modeling. Palaeogeogr Palaeoclimatol Palaeoecol 361–362:49–60

Siddall M, Rohling E, Almogi-Labin A, Hemleben C, Meischner D, Schmelzer I, Smeed DA (2003) Sea-level fluctuations during the last glacial cycle. Nature 423:853–858

Soulet G, Ménot G, Lericolais G, Bard E (2011) A revised calendar age for the last reconnection of the Black Sea to the global ocean. Quat Sci Rev 30:1019–1026

van Andel T, Heath G, Moore T, McGeary DF (1967) Late Quaternary history, climate, and oceanography of the Timor Sea northwestern Australia. Am J Sci 265:737–758

Webster JM, Beaman RJ, Puga-Bernabeu A, Ludman D, Renema W, Wust RAJ, George NPJ, Reimer PJ, Jacobsen GE, Moss P (2012) Late Pleistocene history of turbidite sedimentation in a submarine canyon off the northern Great Barrier Reef, Australia. Palaeogeogr Palaeoclimatol Palaeoecol 331–332:75–89

Whiteway T (2009) Australian Bathymetry and Topography Grid, June 2009. Scale 1:5000000. Geoscience Australia, Canberra

Yokoyama Y, Esat TM (2011) Global climate and sea level: enduring variability and rapid fluctuations over the past 150,000 years. Oceanography 24:54–69

Yokoyama Y, Lambeck K, De Deckker P, Johnston P, Fifield LK (2000) Timing of the Last Glacial Maximum from observed sea-level minima. Nature 406:713–716

Yokoyama Y, Purcell A, Lambeck K, Johnston P (2001a) Shore-line reconstruction around Australia during the Last Glacial Maximum and Late Glacial Stage. Quat Int 83–85:9–18

Yokoyama Y, De Deckker P, Lambeck K, Johnston P, Fifield L (2001b) Sea-level at the Last Glacial Maximum: evidence from northwestern Australia to constrain ice volumes for oxygen isotope stage 2. Palaeogeogr Palaeoclimatol Palaeoecol 165:281–297

Yokoyama Y, Esat TM, Lambeck K (2001c) Coupled climate and sea-level changes deduced from Huon Peninsula coral terraces of the last ice age. Earth Planet Sci Lett 193:579–587

Yokoyama Y, Miyairi Y, Matsuzaki H, Tsunomori F (2007) Relation between acid dissolution time in the vacuum test tube and time required for graphitization for AMS target preparation. Nucl Instrum Meth Phys 259:330–334

Yokoyama Y, Maeda Y, Okuno J, Miyairi Y, Kosuge T (2016a) Holocene Antarctic melting and lithospheric uplift history of the southern Okinawa trough inferred from mid- to late-Holocene sea level in Iriomote Island, Ryukyu, Japan. Quat Int 397:342–348

Yokoyama Y, Anderson JB, Yamane M, Simkins LM, Miyairi Y, Yamazaki T, Koizumi M, Suga H, Kusahara K, Prothro L, Hasumi H, Southon JR, Ohkouchi N (2016b) Widespread collapse of the Ross Ice Shelf during the late Holocene. Proc Natl Acad Sci 113:2354–2359

Yu F, Zong Y, Lloyd JM, Huang G, Leng MJ, Kendrick C, Lamb AL, Yim WWS (2010) Bulk organic d13C and C/N as indicators for sediment sources in the Pearl River delta and estuary, southern China. Estuar Coast Shelf Sci 87:618–630